2003-01-1620

Sound Radiation from a Disk Brake Rotor Using a Semi-Analytical Method

Hyeongill Lee and Rajendra Singh
The Ohio State University

ABSTRACT

Modal sound radiation of a brake rotor is expressed in terms of analytical solutions of a generic thick annular disk having similar geometric dimensions. Finite element method is used to determine structural modes and response. Vibro-acoustic responses such as surface velocities and radiated sound pressures due to a multi-modal excitation are calculated from synthesized structural modes and modal acoustic radiation of the rotor using the modal expansion technique. In addition, acoustic power and radiation efficiency spectra corresponding to a specific force excitation are obtained from the sound pressure data. Accuracy of the new semi-analytical method has been confirmed by purely numerical analyses based on finite element and boundary element models. Our method should lead to an improved understanding of the sound radiation from a brake rotor and strategies to minimize squeal noise radiation could be formulated.

INTRODUCTION

Several structural dynamic models have been used to explain the brake squeal generation mechanism based on the self-excited vibration [1] or modal coupling phenomena [2,3]. Recently, non-linear transient analysis [4,5] and complex eigen-value method [6-9] have been implemented using commercial finite element software. Also, Dunlap et al. [10] investigated squeal noise in various frequency ranges using various approaches and concluded that natural frequency separation between coupled flexural and tangential modes is critical in generating high frequency squeal noise. Most prior studies have focused on the structural dynamics of brake rotors and related components. The acoustic radiation mechanism has not been adequately examined. To fill this void, we investigate sound radiation from a simplified brake rotor in this article. A semi-analytical procedure is proposed that is based on structural eigen-solutions from finite element analysis and analytical modal sound radiation solutions developed for a thick annular disk.

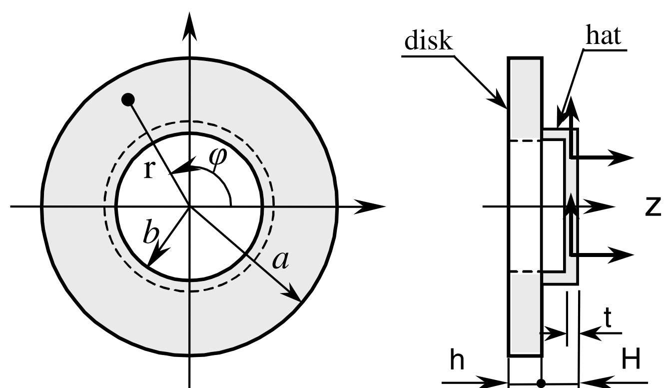

Figure 1. A thick annular disk with a hat structure simulates the brake rotor. Disk is clamped at the inner bolts and free at outer edge

Table 1. Geometric dimensions and material properties of the brake rotor.

Outer radius (a)	151.5 mm
Inner radius (b)	87.5 mm
Radii ratio (β = b/a)	0.54
Disk thickness (h)	31.5 mm
Hat height (H)	24 mm
Hat thickness (t)	6 mm
Density (ρ_d)	7905.9 Kg/m^3
Young's modulus (E)	218 GPa
Poisson's ratio (ν)	0.305

Figure 1 describes the geometric configurations of the rotor example used in this study. In addition, geometric dimensions and material properties are given in Table 1.

OBJECTIVES AND ASSUMPTIONS

Chief objectives of this article are as follows. (1) Develop semi-analytical solutions for sound radiation from modal vibrations of a brake rotor. (2) Introduce a modal synthesis procedure to calculate the vibro-acoustic response to an arbitrary harmonic excitation. (3) Validate proposed analytical procedures using computational vibro-acoustic methods. As evident from Figure 1 and Table 1, disk thickness (h) is not negligible compared to other dimensions of the disk area. Consequently, it is necessary to simultaneously consider both in-plane and out-of-plane vibrations for a complete investigation of the vibro-acoustic characteristics of a brake rotor. Primary assumptions are as follows: (1) Structural and acoustic systems are linear time-invariant systems and complicating effects such as fluid loading and acoustic scattering from the disk edges are negligible. (2) Sound is radiated by only the thick annular disk area and the hat structure of Figure 1 does not contribute to the radiated sound pressure. (3) Boundary conditions for the mounting bolts can be accurately simulated by the ideal clamped boundaries at the same locations.

STRUCTURAL MODAL ANALYSIS

The structural dynamics of the rotor of Figure 1 have been investigated using a finite element model with 2010 solid elements and 3960 nodes [11]. To simulate realistic boundary conditions, clamped nodal restraints have been applied at the locations of mounting bolts. A schematic of this finite element model is given in Figure 2.

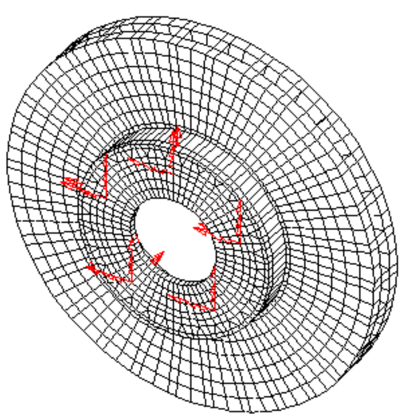

Figure 2. Finite element model of the brake rotor with 2010 solid elements

As many as 44 structural modes up to 16 kHz have been defined in our analysis. Selected natural frequencies and mode shapes are listed in Table 2. In our study, structural modes are described using four modal indices such as m (number of nodal circles), n (number of nodal diameters), q (radial mode index) and l (tangential mode index). Furthermore, structural modes of a brake rotor are categorized into three types: out-of-plane modes described by (m, n), in-plane modes given by (l, q), and combined modes given by (m, n and q). As shown in the table, the q^{th} radial modes are always coupled with out-of-plane modes having the same number of nodal diameters (n) as q, due to the hat structure and clamped boundary conditions.

Table 2. Selected structural modes of the brake rotor.

a. Out-of-Plane Modes (m, n)

Mode no.	1, 2	4, 5	9,10	13
Freq. (Hz)	900	1700	3500	4000
Mode Shape	(0, 1)	(0, 2)	(0, 3)	(1, 0)
	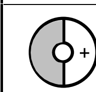	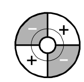	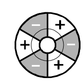	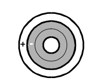

b. In-Plane Modes (l, q)

Mode no.	6	20
Freq. (Hz)	1920	7240
Mode Shape	l = 0	q = 0
	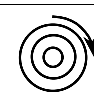	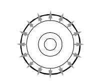

c. Combined Modes (m, n and q)

Mode no.	7, 8	11, 12	18, 19
Freq. (Hz)	2500	3800	7120
Mode Shape	m = 0 n = 1 q = 1 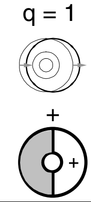	m = 0 n = 1 q = 1 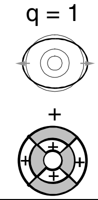	m = 0 n = 1 q = 1 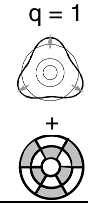

SOUND RADIATION FROM NORMAL MODES OF DISK OR ROTOR

SOUND RADIATION FROM A GENERIC ANNULAR DISK

Lee and Singh [12] have developed an analytical solution for sound radiation from normal modes of a generic thick annular disk using various analytical approaches. According to this study, far-field sound pressure (P) at a given receiver position $r_p(R, \theta, \phi)$ due to out-of-plane modes with m nodal circles and n nodal diameters can be expressed as follows.

$$P_{mn}(R,\theta,\phi) = (1+\cos\theta)P^s_{mn}(R,\theta,\phi) + (1-\cos\theta)P^o_{mn}(R,\theta,\phi)$$
$$P^s_{mn}(R,\theta,\phi) = \frac{\rho_0 c k_{mn} e^{ik_{mn}R}}{2R} e^{-ik_{mn}\frac{h}{2}\cos\theta} \cos n\phi (-i)^{n+1} \mathrm{B}_n[\dot{w}(r)]$$
$$P^o_{mn}(R,\theta,\phi) = -\frac{\rho_0 c k_{mn} e^{ik_{mn}R}}{2R} e^{ik_{mn}\frac{h}{2}\cos\theta} \cos n\phi (-i)^{n+1} \mathrm{B}_n[\dot{w}(r)] \quad (1)$$

Here, ρ_0 is mass density of the acoustic medium, c is the speed of sound in the medium and k_{mn} is the acoustic wave-number of corresponding mode. Also, $\mathrm{B}_n[\dot{w}(r)]$ is Hankel transform of the disk surface velocity that is defined as follows:

$$\mathrm{B}_n[\dot{w}(r)] = \int_0^\infty \dot{w}(r) J_n(k_r r) r dr; \quad k_r = k\sin\theta \quad (2)$$

Numerical and experimental validations confirm the utility of this solution [12]. In addition, Lee and Singh [13] investigated sound radiation from radial modes using a modified cylindrical radiator model. According to this study, far-field sound pressure at $\mathbf{r_p}$ can be expressed by the following equation.

$$P_q(R,\theta,\phi) = P_{qI}(R,\theta,\phi) + P_{qO}(R,\theta,\phi)$$
$$P_{qO}(R,\theta,\phi) = \frac{\rho_0 e^{ik_q R}}{\pi k_q R\sin\theta} |\ddot{u}_{qO}| h \frac{Sinc(k_q \sin\theta\, h/2)(-i)^{q+1}}{H^{1\prime}_q(k_q a \sin\theta)} \times \cos q\phi$$
$$P_{qI}(R,\theta,\phi) = \frac{\rho_0 e^{ik_q R}}{\pi k_q R\sin\theta} |\ddot{u}_{qI}| h \frac{Sinc(k_q \sin\theta\, h/2)(-i)^{q+1}}{H^{2\prime}_q(k_q b \sin\theta)} \times \cos q\phi \quad (3)$$

Here, $|\ddot{u}_{qO}|$ and $|\ddot{u}_{qI}|$ are the acceleration amplitudes on the outer and inner radial surfaces, k_q is the acoustic wave-number of the corresponding mode. Also, H^1_q and H^2_q are the 1st and 2nd kind Hankel functions of order q and Sinc function is defined as Sinc(x) = sin(x)/x. Refer to [13] for the validation of this solution.

SOUND RADIATION FROM A BRAKE ROTOR

As shown in Table 2, mode shapes of pure out-of-plane (flexural) modes of a brake rotor can be expressed with the same modes of a generic annular disk of with identical geometric dimensions. Consequently, sound radiation from these modes can be expressed in terms of the modal sound radiation for the corresponding annular disk. In this study, far-field sound pressure due to the (m, n)th out-of-plane mode is calculated using equation (1). Sound power (Π) for mode (m, n) is calculated from the far-field sound pressure P_{mn} using the following equation.

$$\Pi_{mn} = \langle I_{mn} S_V \rangle_s = \frac{1}{2}\int_0^{2\pi}\int_0^{\pi} \frac{P_{mn}^2}{\rho_0 c_0} R^2 \sin\theta\, d\theta\, d\phi \quad (4)$$

Here, I_{mn} is the acoustic intensity on a sphere S_v where S_v is the control surface. The modal radiation efficiency σ_{mn} of an annular disk is determined from Π_{mn} as follows where $<|\dot{w}_{mn}|^2>_{t,s}$ is the spatially averaged mean-square velocity on the two normal surfaces of an annular disk.

$$\sigma_{mn} = \frac{\Pi_{mn}}{<|\dot{w}_{mn}|^2>_{t,s}};$$
$$<|\dot{w}_{mn}|^2>_{t,s} = \frac{1}{2\pi(a^2-b^2)}\int_b^a\int_0^{2\pi} \dot{W}^2 d\varphi\, dr \quad (5)$$

Next we consider, the qth radial modes that are always coupled with (m = 0, n = q) or (m = 1, n = q) out-of-plane modes except for the q = 0 radial mode. Since the thickness of disk (h) is beyond the thin plate theory limit, sound radiation from in-plane (radial) modes should be included in the calculation of total sound radiation from such modes. Modal velocity distributions on the normal and radial surfaces have been defined from numerically estimated natural frequencies and modes shapes. Consequently, the total far-field sound pressure at a given receiver position is expressed as sum of sound pressure from radial surfaces (due to the radial mode as calculated by equation (3)) and that from normal surfaces (due to the out-of-plane mode as given by equation (1)). Modal acoustic power for combined mode (m, n, q) can be obtained using an equation similar to equation (4) from the total sound pressure. In addition, modal radiation efficiencies for these combined modes have been obtained using following equation.

$$\sigma_{mnq} = \frac{\Pi_{mnq}}{<|\dot{v}_{mnq}|^2>_{t,s}} \quad (6)$$

In this case, $<|\dot{v}_{mnq}|^2>_{t,s}$ should be calculated and averaged over the entire radiating surface. It can be obtained using the following equation.

$$\left\langle |\dot{v}_{mnq}|^2 \right\rangle_{t,s} = \frac{1}{4\pi h(a+b) + 2\pi(a^2-b^2)} \times \left\{ \int_{-h/2}^{h/2} \int_0^{2\pi(a+b)} \dot{U}^2 dl\, dz + \int_b^a \int_0^{2\pi} \dot{W}^2 d\varphi\, dr \right\} \qquad (7)$$

For pure in-plane modes, the far-field sound pressure can be calculated by using only equation (3). Acoustic power and radiation efficiency can be obtained by the same expressions as equations (4) and (6). Since normal surfaces do not contribute to the modal sound pressure, $<|\dot{v}|^2>_{t,s}$ should be calculated over radial surfaces only using the following equation.

$$\left\langle |\dot{v}_q|^2 \right\rangle_{t,s} = \frac{1}{4\pi h(a+b)} \int_{-h/2}^{h/2} \int_0^{2\pi(a+b)} \dot{U}^2 dl\, dz \qquad (8)$$

The accuracy of this procedure has been confirmed through a comparison with a purely numerical analysis in terms of the directivity patterns, sound powers and radiation efficiencies. In the numerical analysis, velocities on the rotor surface are calculated from predicted natural frequencies and mode shapes. And, sound radiation data have been calculated using uncoupled, direct, exterior, and unbaffled boundary element analyses [14].

Mode	BEM	Analytical
m =0 n = 2	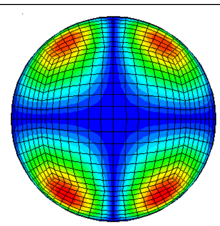	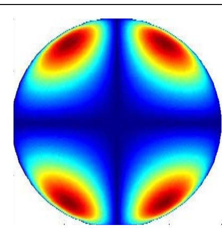
m = 1 n = 2 q = 2	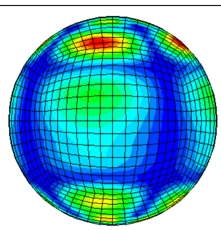	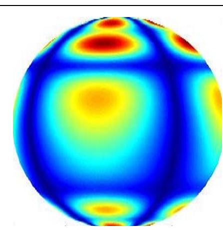
q = 0	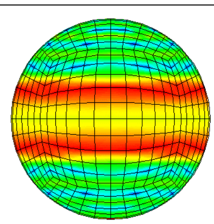	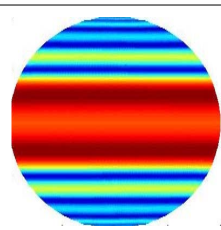

Figure 3. Directivity patterns for selected modes.

The analytical directivity patterns for selected modes are compared with numerical predictions in Figure 3. As one can see, analytical and numerical directivity patterns for 3 types of modes are consistent with each other. In addition to the directivity patterns, modal sound powers and radiation efficiencies are listed in Table 3. Like the directivity patterns, modal sound radiation data from analytical solutions match numerical data quite well. Therefore, analytical modal radiation basis can be used to calculate sound radiation from a brake rotor when excited by a multi-directional harmonic force. This procedure is explained in the next section.

Table 3. Sound powers and radiation efficiencies for selected modes.

Structural Mode					Sound Power (dB re 1pW)		Radiation Efficiency (σ)	
Type	Indices				Anal-ytical	BEM	Anal-ytical	BEM
	m	n	q	l				
Out Of Plane	0	1	-	-	74	72	0.15	0.05
	0	2	-	-	83	86	0.37	0.44
	0	3	-	-	92	92	0.77	0.56
In Plane	-	-	-	0	0	0	-	-
	-	-	0	-	99	99	0.52	0.69
Com-bined	0	1	1	-	87	88	0.40	0.31
	1	2	2	-	91	91	0.43	0.34
	1	3	3	-	96	95	0.71	0.44

VIBRO-ACOUSTIC RESPONSE TO A MULTI-DIRECTIONAL HARMONIC FORCE

If a rotor is excited by a multi-directional harmonic force of arbitrary frequency, several in-plane and out-of-plane modes are simultaneously excited. Based on the modal expansion technique, velocity distribution (**v**) on the disk surfaces can be expressed in terms of the structural modes of the disk.

$$\begin{aligned} \{v\} &= \{\eta\}^T \{\Phi\} \\ \{\Phi\} &= \{\Phi_1, \Phi_2, \Phi_3, \cdots, \Phi_{44}\} \\ \{\eta\} &= \{\eta_1, \eta_2, \eta_3, \cdots, \eta_{44}\} \end{aligned} \qquad (9)$$

where Φ_j is the j[th] velocity modal vector of the disk and η_i is the corresponding modal participation factor. Structural modal participation factors due to a harmonic force with frequency ω can be obtained from the modal data set (natural frequencies, mode shapes, and damping ratios) as follows:

$$\eta_j = \sum_j \frac{\Phi_j(r_f, \varphi_f)\Phi_j^T(r, \varphi)}{(1-\omega^2/\omega_j^2) + i2\varsigma_i(\omega/\omega_j)} \tag{10}$$

Lee and Singh [15] expressed the far-field sound pressure from a thin annular disk due to a multi-modal excitation using structural modal participation factors and modal sound pressures. Applying the same procedure to this problem, the far-field pressure on the sphere (S_V) surrounding the disk due to surface velocity of equation (9) is expressed as follows:

$$\begin{aligned} P &= \{\eta\}^T\{\Gamma\} \\ \{\Gamma\} &= \{\Gamma_1, \Gamma_2, \Gamma_2, \Gamma_3, \cdots, \Gamma_{44}\} \end{aligned} \tag{11}$$

where, Γ_j is the modal sound pressure for the j^{th} mode obtained from equation (1) or (3). Sound power (Π) from the rotor due to an arbitrary harmonic force (f) is also calculated from far-field sound pressures, on a sphere surrounding the disk, as follows:

$$\Pi = \langle IS_V \rangle_s = \frac{1}{2}\int_0^{2\pi}\int_0^{\pi} \frac{P^2}{\rho_0 c} R^2 \sin\theta \, d\theta \, d\phi \tag{12}$$

Corresponding radiation efficiency (σ) is calculated using Π from equation (12) and $<|\dot{v}|^2>_{t,s}$ that is obtained from velocity on the total radiating surfaces using an equation similar to equation (7). As in the case of modal sound radiation, vibro-acoustic responses to a multi-directional force are obtained using the proposed analytical procedure and compared with prediction of a numerical analysis. In the purely computational analysis, structural responses for the excitation are obtained from the forced vibration analysis with the finite element model and acoustic responses are obtained by boundary element analysis given structural velocities.

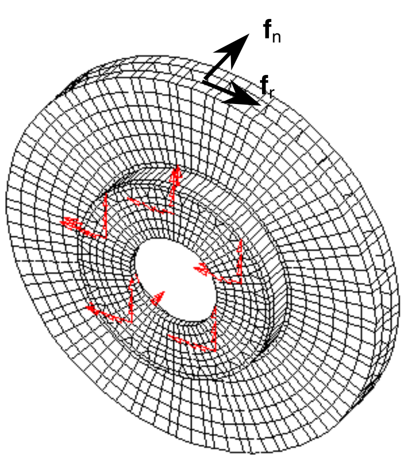

Figure 4. Finite element model used for forced vibration analysis given a multi-directional harmonic force.

In this example, unit harmonic forces in the normal and tangential directions are applied in the mid-plane of rotor at $\varphi = \pi/2$ as shown in Figure 4. Far-field sound pressure spectra p

(ω) are obtained using above procedure from 0.8 to 8 kHz. Results for two receiver positions $\mathbf{r}_{p1}$ (R = 1m, θ = 0, ϕ = 0) and $\mathbf{r}_{p2}$ (R = 1m, $\theta = \pi/4$, ϕ = 0) are compared with purely numerical results in Figure 5. As shown in Figure 5, p(ω) from analytical approach matches purely computational prediction quite well for both cases. Furthermore, these results depend on the receiver positions indicating that the source is highly directive. In addition, sound power and radiation efficiency spectra have been determined. A comparison of analytically obtained spectra and numerical results is given in Figure 6. Also, analytical acoustic power and radiation efficiency spectra show relatively good agreement especially below 5 kHz. As seen from Figures 5 and 6, the proposed analytical procedure has sufficient accuracy in calculating the sound radiation due to a harmonic force. Sound pressure at a given receiver position, sound power or radiation efficiency for a given harmonic excitation can be easily calculated using this process. Furthermore, this procedure could be easily extended to multi-location or multi-frequency excitation cases by considering the modal participation factors. Even though numerical structural modal data have been used, experimental results could be utilized instead of numerical data.

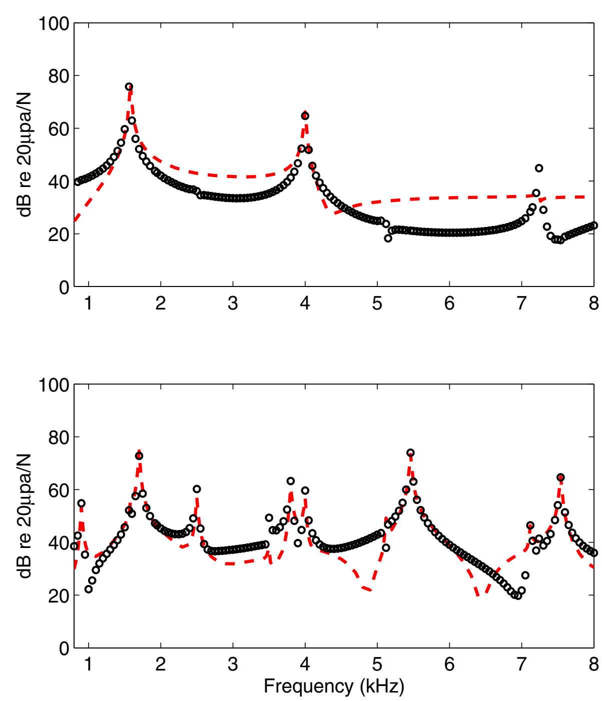

Figure 5. Far-field sound pressure spectra p(ω) for selected receiver positions (a) $\mathbf{r}_{p1}$ and (b) $\mathbf{r}_{p2}$. Key: Analytical °°°•; Computed using BEM ----.

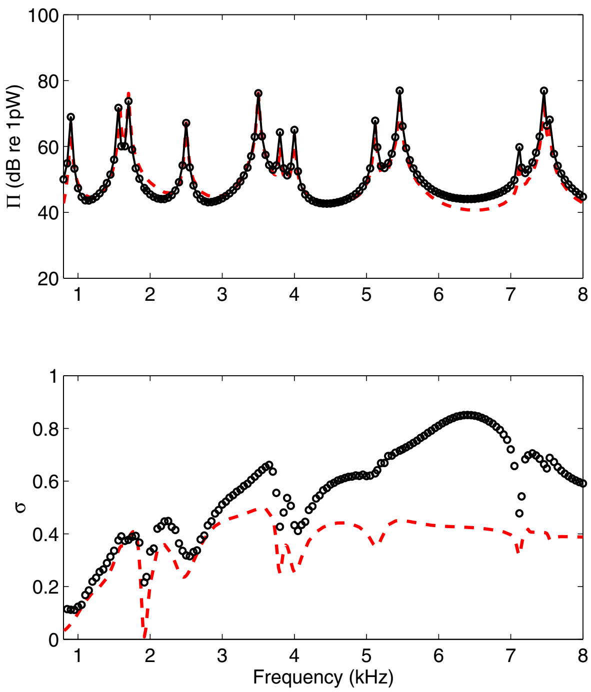

Figure 6. Acoustic power $\Pi(\omega)$ and radiation efficiency spectra $\sigma(\omega)$ of the brake rotor. Key: Analytical °°°; Computed using BEM ----.

COMPARISON WITH EXPERIMENTAL RESULTS FOR A FREE-FREE GENERIC DISK

Finally, we validate the analytical solutions for a generic disk that are employed to describe the modal radiation of a brake rotor. Table 4 compares predicted and measured structural and acoustic characteristics for a free - free generic annular disk that has identical geometric dimensions as the sample rotor. Also, computed results are given for reference.

Table 4. Vibro-acoustic characteristics for a generic disk. (a) Sound radiation, (b) Structural characteristics

(a)

Mode			Sound Power (dB re 1pW)			Radiation Efficiency (σ)		
m	n	q	Anal-ytical	Mea-sured	BEM	Anal-ytical	Mea-sured	BEM
1	1	-	71.6	70.1	70.7	1.08	0.77	0.75
0	3	-	76.2	75.3	76.3	1.01	0.81	1.01
-	-	2	66.0	60.0	66.5	0.63	0.14	0.63
-	-	3	67.5	62.0	67.5	0.79	0.22	0.85

(b)

Mode			Natural Frequency (kHz)		
m	n	q	Analytical	Measured	FEM
1	1	-	5.07	4.76	4.61
0	3	-	3.68	3.48	3.47
-	-	2	2.86	2.83	2.89
-	-	3	6.91	6.86	6.99

CONCLUSION

Modal sound radiation from a brake rotor is successfully calculated by using a semi-analytical procedure based on structural modal response yielded by a numerical code and analytical solution for sound radiation from a generic thick annular disk. Vibro-acoustic response for a harmonic force is synthesized quite reliably from modal sound radiation data and the structural modal participation factors using the modal expansion technique. Our procedure could utilize either computational or experimental modal data such as natural frequencies, mode shapes and modal damping ratios. The modal expansion technique used to calculate sound radiation due to a harmonic excitation could be easily generalized to multi-locations or multi-frequencies excitations. One would, however, need to define additional modal participation factor vectors. Effects of geometric modifications on vibro-acoustic characteristics can be easily investigated using this procedure. Also, this procedure could be combined with pre-developed methods using numerical and experimental approaches. Finally, it is possible to develop vibro-acoustic design guidelines using this procedure.

REFERENCES

1. H. Murakami, N. Tsunada and T. Kitamura, "A Study Concerned with a Mechanism of Disc-Brake Squeal," SAE Paper # 841233.
2. W. V. Nack and A. M, Joshi, "Friction Induced Vibration: Brake Moan," SAE Paper # 951095.
3. D. N. Herting, MSC/NASTRAN Advanced Dynamic Analysis User's Guide, pp. 157-173, 1997.
4. Y. K. Hu, and L. I. Nagy, "Brake Squeal Analysis by Using Nonlinear Transient Finite Element Method," SAE Paper # 971510.
5. O. N. Hamzeh, W. W. Tworzydlo, H. J. Chang and S. T. Fryska, "Analysis of Friction-Induced Instabilities in a Simplified Aircraft Brake, SAE Paper # 1999-01-3404.
6. G. D. Liles, "Analysis of Disc Brake Squeal Using Finite Element Methods," SAE Paper # 891150.

7. G. Dihua and J. Dongying, “A Study on Disc Brake Squeal using Finite Element Methods,” SAE Paper # 980597.
8. T. Hamabe, I. Yamazaki, K, Yamada, H. Matsui, S. Nakagawa and M. Kawamura, “Study of a Method for Reducing Drum Brake Squeal,” SAE Paper # 1999-01-0144.
9. S. W. Kung, K. B. Dunlap and R. S. Ballinger, “Complex Eigenvalue Analysis for Reducing Low Frequency Squeal,” SAE Paper # 2000-01-0444.
10. K. B. Dunlap, M. A. Riehle and R. E. Longhouse, “An Investigative Overview of Automotive Disc Brake noise” SAE Paper # 1999-01-0142.
11. I-DEAS User’s manual version 8.2, SDRC, USA, 2000.
12. H. Lee and R. Singh, “Acoustic radiation from out-of-plane modes of an annular disk based on thick plate theory”, submitted to the Journal of Sound and Vibration, 2002.
13. H. Lee and R. Singh, “Acoustic radiation from radial modes of a thick annular disk”, submitted to the Journal of Sound and Vibration, 2002.
14. SYSNOISE User’s manual Version 5.4, NIT, Belgium, 1999.
15. M. R. Lee and R. Singh, “Analytical formulations for annular disk sound radiation using structural modes”, Journal of the Acoustical Society of America 95(6), pp. 3311-3323, 1994.

LIST OF SYMBOLS

a	outer radius of annular disk
b	inner radius of annular disk
c_0	speed of sound in the acoustic medium
$f_n(t)$, $f_r(t)$	dynamic force on rotor
F	amplitude of applied force
h	disk thickness
H	Hat height
i	$\sqrt{-1}$
I	acoustic intensity at a field point
k	acoustic wave number
k_q	structural wave number in z direction
l	tangential mode index
m	number of nodal circle
n	number of modal diameters
R, θ, φ	spherical coordinates for receiver positions
q	radial mode index
$\mathbf{r}_f$	position vector of force f(t) on rotor
$\mathbf{r}_p$	position vector of sound pressure
$\mathbf{r}_s$	position vector of source
S_o	surface of sound source
S_v	boundary surface of acoustic control volume
$\ddot{u}_{qI}, \ddot{u}_{qO}$	acceleration on inner and outer radial surfaces
$\dot{U}$	spatially-dependent radial velocity of disk
V	acoustic control volume
w	transverse displacement of rotor
W	spatial dependent transverse displacement
η	structural modal participation factor vector
Γ	modal sound pressure of rotor
Π	acoustic power
Π_{mn}, Π_q	acoustic power from the modal vibrations
ρ_0	mass density of acoustic medium
ρ_d	mass density of the rotor
$\sigma_{mn,}$ σ_q	sound radiation efficiency of normal modes
φ	azimuthal angle of rotor
Φ	velocity modal vector of rotor
ω_j	natural frequencies of rotor
ζ_j	modal damping ratios of rotor

Subscripts

d	rotor
j	mode number
I	inner radial edge
l	tangential mode index
m,n	out-of-plane mode indices
O	outer radial edge
p	observation point in far field
q	radial mode index
s	source (radiator)
φ	circumferential direction of rotor

Superscripts

1	first kind
2	second kind

Abbreviations

BEM	boundary element method
FEM	finite element method

ACKNOWLEDGMENTS

This project has been supported by the Center for Automotive Research Industrial Consortium and the sponsors include Bosch, CRF Fiat, Delphi Chassis, Dow Automotive, Ford, Edison Welding Institute, General Motors and LuK over the 1999 – 2001 period.

CONTACT

www.AutoNVH.org